Multiconductor Transmission Line Models for Modal Transmission Schemes

Frédéric Broydé, *Senior Member, IEEE*, and Evelyne Clavelier, *Senior Member, IEEE*

***Abstract*— We investigate modal transmission schemes used to reduce echo and internal crosstalk in a multichannel link using an untransposed multiconductor interconnection. The core of such a modal transmission scheme is an appropriate multiconductor transmission line (MTL) model of the interconnection. The standard theory of modal signaling, which emphasizes modal voltages, modal currents, and associated eigenvectors is summarized. Then, we present new results of MTL theory: three theorems on generalized associated eigenvectors and two high-frequency approximations. These results are needed to explain an assumption used in some modal transmission schemes.**

***Index Terms*— Crosstalk, interconnection, multiple-input and multiple-output (MIMO) systems, signal integrity, transmission.**

I. Introduction

In a linear multichannel electrical link used for signal transmission, such as the link shown in Fig. 1, we can consider two endogenous transmission impairments: echo, the detrimental phenomenon by which a signal sent or received at an end of the link, in one of the channels, is followed by the reception of a delayed noise on the same channel, at the same end of the link; and internal crosstalk, the detrimental phenomenon by which a signal sent in one of the channels produces noise in another channel. Detrimental interactions may also exist between the link and other circuits of the device in which it is built; the resulting crosstalk between one or more channels of the link and such other circuits is referred to as external crosstalk.

In modal transmission, each channel is allocated to a propagation mode of a multiconductor interconnection [1]. A single channel differential link uses the differential mode of a balanced pair for signal transmission: this is the simplest example of modal signaling. In the ideal telephone system of the beginning of the 20th century, where the interconnection comprises multiple balanced pairs, transposition (i.e., frequent permutations of the conductors) is used to obtain that, at voice frequency, a differential mode in one of the balanced pairs approximately corresponds to a propagation mode [2], [3]. This paper is about the theoretical foundation of modal signaling schemes intended to reduce internal crosstalk in a multichannel link using an untransposed interconnection.

Manuscript received March 27, 2012; revised July 7, 2012 and October 8, 2012; accepted October 15, 2012. Date of publication January 14, 2013; date of current version January 31, 2013. Recommended for publication by Associate Editor A. Maffucci upon evaluation of reviewers' comments.

The authors are with Excem, Maule 78580, France (e-mail: fredbroyde@eurexcem.com; eclavelier@eurexcem.com).

Color versions of one or more of the figures in this paper are available online at http://ieeexplore.ieee.org.

Digital Object Identifier 10.1109/TCPMT.2012.2227259

The link considered in this paper comprises a multiconductor interconnection, that is, a physical device having $n \geq 2$ transmission conductors (TCs) and a reference conductor or ground conductor (GC). We need to distinguish between crosstalk and TC-to-TC coupling. TC-to-TC coupling collectively designates mutual capacitance between the TCs and mutual impedance between loops each comprising one of the TCs and the GC. In a multichannel single-ended link where a single TC is allocated to each channel, TC-to-TC coupling causes internal crosstalk, so that increasing the distances between the TCs to reduce TC-to-TC coupling is one of the standard crosstalk reduction techniques. In a single-channel differential link where two TCs form a balanced pair, TC-to-TC coupling does not cause internal crosstalk and is advantageous in several respects. However, in a multichannel differential link using a planar arrangement of untransposed pairs, TC-to-TC coupling between the TCs of different pairs will cause internal crosstalk. Thus, a sufficient spacing between the pairs is necessary. As a consequence, in a link built in a single layer of the substrate of a multichip module (MCM) or printed circuit board providing $m \geq 2$ channels for high-speed digital transmission, $m-1$ wide spacings are needed to obtain a sufficiently low internal crosstalk, in the cases of single-ended signaling and of differential signaling [4, Sec. 7.2].

In the case of a modal signaling scheme using a uniform interconnection, such as the ZXtalk method, TC-to-TC coupling is not a cause of crosstalk [1], [5]–[7]. Thus, modal signaling can be used to build multichannel links having a narrow spacing between the TCs and a reduced number of conductors and leads compared to multichannel differential links.

The core of any modal signaling scheme is a suitable multiconductor transmission line (MTL) model for the interconnection, and the definition of the modes used for signaling. The theory used in the initial definition of the ZXtalk method emphasized the concept of total decoupling and the role of associated eigenvectors, because only modes providing total decoupling have the desired property of independent propagation, and associated eigenvectors were shown to provide total decoupling. This theory is summarized in Section II. A concept of generalized associated eigenvectors and three theorems about them are proven in Section III, where the second and third theorems are new. These results are important for modal signaling schemes because they tell us how we can build all sets of mode providing total decoupling. They also reveal the properties of two possible choices of generalized associated eigenvectors. Sections IV and V are new developments in which we explore approximations applicable

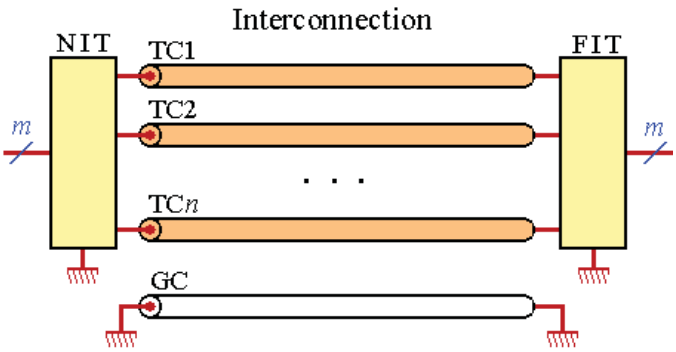

Fig. 1. Point-to-point link providing m channels, consisting of an interconnection, NIT, and FIT. The interconnection has n TCs and a GC.

to low and to high frequencies and compare high-frequency approximations. This analysis of approximations is necessary to justify a property, which was previously stated and used, but never proven: it is usually possible to consider that, when computing the characteristic impedance matrix and a transition matrix from modal electrical variables to natural electrical variables, the losses are negligible in some frequency band [1, Sec. VII], [6, Sec. IV]. This approximation is not needed for circuit simulation, but it is essential for the design of links implementing a modal signaling scheme at high frequency, because it reduces the complexity of the near-end interface and termination device (NIT) and of the far-end interface and termination device (FIT).

II. Definitions and Basic Properties

In this section, we mainly summarize [8, Secs. 4–7], and we use the same notations. We consider the link shown in Fig. 1, providing m channels and comprising: an interconnection having n TCs and a GC, where $n \geq m$, a NIT and a FIT. The GC is used as a reference for voltage measurements. We number the TCs from 1 to n, and we define:

1) the curvilinear abscissa z, the interconnection extending from $z = 0$ to $z = \mathcal{L}$;
2) the natural current i_j as the current flowing on the TC j, toward $z = \mathcal{L}$;
3) the natural voltage v_j as the voltage between the TC j and the GC;
4) the column vector $\mathbf{i}$ of the natural currents $i_1, \ldots, i_n$, which depends on z;
5) the column vector $\mathbf{v}$ of the natural voltages $v_1, \ldots, v_n$, which depends on z.

We shall only consider frequency domain quantities. We assume that the interconnection can be modeled as a MTL. The $(n + 1)$-conductor MTL model uses a per-unit-length (p.u.l.) impedance matrix $\mathbf{Z}'$ and a p.u.l. admittance matrix $\mathbf{Y}'$, which are used in the telegrapher's equations

$$\begin{cases} \frac{d\mathbf{v}}{dz} = -\mathbf{Z}'\mathbf{i} \\ \frac{d\mathbf{i}}{dz} = -\mathbf{Y}'\mathbf{v}. \end{cases} \tag{1}$$

$\mathbf{Z}'$ and $\mathbf{Y}'$ are frequency-dependent symmetric matrices of size $n \times n$. $\mathbf{Z}'$ and $\mathbf{Y}'$ each must represent a passive linear system. Thus, their real part is positive semidefinite [9, Sec. 7.1]. We shall assume that $\mathbf{Z}'$ and $\mathbf{Y}'$ are invertible. The MTL is lossless if and only if $\mathbf{Z}' = j\omega\mathbf{L}'$ and $\mathbf{Y}' = j\omega\mathbf{C}'$ where $\mathbf{L}'$ and $\mathbf{C}'$ are real matrices of size $n \times n$. In this case, $\mathbf{L}'$ and $\mathbf{C}'$ must be frequency independent. In this paper, uniform means independent of z. The MTL is said to be uniform if $\mathbf{Z}'$ and $\mathbf{Y}'$ are uniform.

Assuming a uniform MTL, we can derive two second order differential equations

$$\begin{cases} \frac{d^2\mathbf{v}}{dz^2} - \mathbf{Z}'\mathbf{Y}'\mathbf{v} = \mathbf{0} \\ \frac{d^2\mathbf{i}}{dz^2} - \mathbf{Y}'\mathbf{Z}'\mathbf{i} = \mathbf{0}. \end{cases} \tag{2}$$

$\mathbf{Z}'\mathbf{Y}'$ and $\mathbf{Y}'\mathbf{Z}'$ are similar [9, Sec. 1.3.20]. We shall assume that $\mathbf{Z}'\mathbf{Y}'$, or equivalently $\mathbf{Y}'\mathbf{Z}'$, is diagonalizable. In this case, there exist two invertible matrices $\mathbf{T}$ and $\mathbf{S}$ such that

$$\begin{cases} \mathbf{T}^{-1}\mathbf{Y}'\mathbf{Z}'\mathbf{T} = \Gamma^2 \\ \mathbf{S}^{-1}\mathbf{Z}'\mathbf{Y}'\mathbf{S} = \Gamma^2 \end{cases} \tag{3}$$

where

$$\Gamma = \mathrm{diag}_n(\gamma_1, \ldots, \gamma_n) \tag{4}$$

is the diagonal matrix of order n of the propagation constants γ_i, chosen with an argument lying in $]-\pi/2, \pi/2]$, so that the γ_i are principal square roots. $\mathbf{T}$ and $\mathbf{S}$ define a modal transform for the natural currents and for the natural voltages, respectively. We can also say that $\mathbf{T}$ and $\mathbf{S}$ are transition matrices from modal electrical variables to natural electrical variables. The column vectors of $\mathbf{S}$ (respectively, of $\mathbf{T}$) are defined as linearly independent eigenvectors of $\mathbf{Z}'\mathbf{Y}'$ (respectively, of $\mathbf{Y}'\mathbf{Z}'$). Consequently, $\mathbf{S}$ and $\mathbf{T}$ are not uniquely defined by (3). We write

$$\begin{cases} \mathbf{v} = \mathbf{S}\mathbf{v}_M \\ \mathbf{i} = \mathbf{T}\mathbf{i}_M \end{cases} \tag{5}$$

where we use $\mathbf{i}_M$ to denote the vector of the n modal currents $i_{M1}, \ldots, i_{Mn}$; we use $\mathbf{v}_M$ to denote the vector of the n modal voltages $v_{M1}, \ldots, v_{Mn}$; we call $\mathbf{S}$ the transition matrix from modal voltages to natural voltages; and we call $\mathbf{T}$ the transition matrix from modal currents to natural currents. The eigenvoltages (the columns of $\mathbf{S}$) need not be orthogonal and the eigen-currents (the columns of $\mathbf{T}$) need not be orthogonal [1, Sec. VI], [8, Sec. 7].

Using (3) and (5), we find that (2) is equivalent to

$$\begin{cases} \frac{d^2\mathbf{v}_M}{dz^2} - \Gamma^2\mathbf{v}_M = 0 \\ \frac{d^2\mathbf{i}_M}{dz^2} - \Gamma^2\mathbf{i}_M = 0 \end{cases} \tag{6}$$

where each vector equation contains n decoupled scalar equations. For a function $f(u)$ of the variable $u \in \mathbb{C}$ and a diagonal matrix $\mathrm{diag}_n(a_1, \ldots, a_n)$, we define $f(\mathrm{diag}_n(a_1, \ldots, a_n)) = \mathrm{diag}_n(f(a_1), \ldots, f(a_n))$. Using this definition, the general solution of (6) is

$$\begin{cases} \mathbf{v}_M = \mathbf{v}_{M+} + \mathbf{v}_{M-} \\ \mathbf{i}_M = \mathbf{i}_{M+} + \mathbf{v}_{M-} \end{cases} \tag{7}$$

where

$$\begin{cases} \mathbf{v}_{M+} = e^{-z\Gamma}\mathbf{v}_{M0+} \\ \mathbf{i}_{M+} = e^{-z\Gamma}\mathbf{i}_{M0+} \end{cases} \quad \text{and} \quad \begin{cases} \mathbf{v}_{M-} = e^{z\Gamma}\mathbf{v}_{M0-} \\ \mathbf{i}_{M-} = e^{z\Gamma}\mathbf{i}_{M0-} \end{cases} \tag{8}$$

where $\mathbf{v}_{M0+}$, $\mathbf{v}_{M0-}$, $\mathbf{i}_{M0+}$, and $\mathbf{i}_{M0-}$ are z-independent vectors depending on the boundary conditions at $z = 0$ and $z = \mathcal{L}$. We find that $\mathbf{v}_{M+}$ is the column vector of the modal voltages traveling toward the far end, $\mathbf{i}_{M+}$ is the column vector of the modal currents traveling toward the far end, $\mathbf{v}_{M-}$ is the column vector of the modal voltages traveling toward the near end, and $\mathbf{i}_{M-}$ is the column vector of the modal currents traveling toward the near end. Thus, for any $\alpha \in \{1, \ldots, n\}$, a modal current $i_{M\alpha}$ and a modal voltage $v_{M\alpha}$ may propagate with the propagation constant γ_α toward the far end, or with the opposite propagation constant $-\gamma_\alpha$ toward the near end.

Using (5) in (6) and (7), we find that the general solution of (2) is

$$\begin{cases} \mathbf{v} = \mathbf{v}_+ + \mathbf{v}_- \\ \mathbf{i} = \mathbf{i}_+ + \mathbf{v}_- \end{cases} \tag{9}$$

where

$$\begin{cases} \mathbf{v}_+ = \mathbf{S}e^{-z\Gamma}\mathbf{v}_{M0+} \\ \mathbf{i}_+ = \mathbf{T}e^{-z\Gamma}\mathbf{i}_{M0+} \end{cases} \text{ and } \begin{cases} \mathbf{v}_- = \mathbf{S}e^{z\Gamma}\mathbf{v}_{M0-} \\ \mathbf{i}_- = \mathbf{T}e^{z\Gamma}\mathbf{i}_{M0-}. \end{cases} \tag{10}$$

Though (2) and (6) are direct consequences of (1), they are not equivalent to (1) because they do not contain the relationships between $\mathbf{i}$ and $\mathbf{v}$ in (1). It is possible to write these relationships using the modal characteristic impedance matrix $\mathbf{Z}_{MC}$ or the characteristic impedance matrix $\mathbf{Z}_C$. In order to define these quantities, we need to show that

$$\begin{aligned} \Gamma^{-1}\mathbf{S}^{-1}\mathbf{Z}'\mathbf{T} &= \Gamma\mathbf{S}^{-1}\mathbf{Y}'^{-1}\mathbf{T} \\ &= \mathbf{S}^{-1}\mathbf{Y}'^{-1}\mathbf{T}\Gamma = \mathbf{S}^{-1}\mathbf{Z}'\mathbf{T}\Gamma^{-1}. \end{aligned} \tag{11}$$

A simple but incorrect proof of (11) assumes that there exist solutions of (1) in the form $\mathbf{v} = \mathbf{v}_+$ and $\mathbf{i} = \mathbf{i}_+$ where $\mathbf{i}_+$ is arbitrary. The following proof seems new and does not use this assumption.

Proof: We have $\mathbf{Y}'\ \mathbf{Z}' = \mathbf{Z}'^{-1}\mathbf{Z}'\ \mathbf{Y}'\ \mathbf{Z}'$. By (3), we find $\mathbf{T}\ \Gamma^2\ \mathbf{T}^{-1} = \mathbf{Z}'^{-1}\ \mathbf{S}\ \Gamma^2\ \mathbf{S}^{-1}\ \mathbf{Z}'$. This invertible and diagonalizable matrix has a unique principal matrix square root, defined in the Appendix as its image under the primary matrix function associated with the complex-valued principal square root. This principal matrix square root is independent of the diagonalization used to compute it, so that we have $\mathbf{T}\ \Gamma\ \mathbf{T}^{-1} = \mathbf{Z}'^{-1}\ \mathbf{S}\ \Gamma\ \mathbf{S}^{-1}\ \mathbf{Z}'$. This can be written $\Gamma^{-1}\ \mathbf{S}^{-1}\mathbf{Z}'\ \mathbf{T}\ \Gamma\ \mathbf{T}^{-1} = \mathbf{S}^{-1}\mathbf{Z}'$, so that we obtain $\Gamma^{-1}\ \mathbf{S}^{-1}\mathbf{Z}'\ \mathbf{T} = \mathbf{S}^{-1}\mathbf{Z}'\ \mathbf{T}\ \Gamma^{-1}$. This is one of the equalities of (11). Using (3) one more time, we obtain $\Gamma^{-1}\ \mathbf{S}^{-1}\ \mathbf{Z}' = \Gamma\ \mathbf{S}^{-1}\mathbf{Y}'^{-1}$ and $\mathbf{Z}'\ \mathbf{T}\ \Gamma^{-1} = \mathbf{Y}'^{-1}\ \mathbf{T}\ \Gamma$, which allow us to obtain (11). ■

The modal characteristic impedance matrix $\mathbf{Z}_{MC}$ is given by

$$\begin{aligned} \mathbf{Z}_{MC} &= \Gamma^{-1}\mathbf{S}^{-1}\mathbf{Z}'\mathbf{T} = \Gamma\mathbf{S}^{-1}\mathbf{Y}'^{-1}\mathbf{T} \\ &= \mathbf{S}^{-1}\mathbf{Y}'^{-1}\mathbf{T}\Gamma = \mathbf{S}^{-1}\mathbf{Z}'\mathbf{T}\Gamma^{-1}. \end{aligned} \tag{12}$$

$\mathbf{Z}_{MC}$ depends on the choice of $\mathbf{S}$ and $\mathbf{T}$. By (11), $\mathbf{S}^{-1}\ \mathbf{Y}'^{-1}\mathbf{T}$ commutes with Γ. Thus, by [10, Sec. 6.2.9], it commutes with $e^{-z\Gamma}$ and $e^{z\Gamma}$. Thus, $\mathbf{Z}_{MC}$ commutes with Γ, $e^{-z\Gamma}$, and $e^{z\Gamma}$. It can easily be shown that

$$\begin{cases} \mathbf{v}_{M+} = \mathbf{Z}_{MC}\mathbf{i}_{M+} \\ \mathbf{v}_{M-} = -\mathbf{Z}_{MC}\mathbf{i}_{M-}. \end{cases} \tag{13}$$

The characteristic impedance matrix $\mathbf{Z}_C$ is given by

$$\begin{aligned} \mathbf{Z}_C &= \mathbf{S}\mathbf{Z}_{MC}\mathbf{T}^{-1} = \mathbf{S}\Gamma^{-1}\mathbf{S}^{-1}\mathbf{Z}' = \mathbf{S}\Gamma\mathbf{S}^{-1}\mathbf{Y}'^{-1} \\ &= \mathbf{Y}'^{-1}\mathbf{T}\Gamma\mathbf{T}^{-1} = \mathbf{Z}'\mathbf{T}\Gamma^{-1}\mathbf{T}^{-1}. \end{aligned} \tag{14}$$

We observe that $\mathbf{S}\ \Gamma\ \mathbf{S}^{-1}$ is the image of $\mathbf{S}\ \Gamma^2\ \mathbf{S}^{-1}$ under the principal matrix square root defined in the Appendix. This principal matrix square root is unique and independent of the choice of $\mathbf{S}$ used to compute it. For the same reason, $\mathbf{S}\ \Gamma^{-1}\ \mathbf{S}^{-1}$, $\mathbf{T}\ \Gamma\ \mathbf{T}^{-1}$, or $\mathbf{T}\ \Gamma^{-1}\ \mathbf{T}^{-1}$ are independent of the choice of $\mathbf{S}$ and $\mathbf{T}$. Thus, $\mathbf{Z}_C$ is unique and does not depend on the choice of $\mathbf{S}$ and $\mathbf{T}$. Using (10) and (13), we obtain

$$\begin{cases} \mathbf{v}_+ = \mathbf{Z}_C\mathbf{i}_+ \\ \mathbf{v}_- = -\mathbf{Z}_C\mathbf{i}_-. \end{cases} \tag{15}$$

A matched termination has an impedance matrix equal to $\mathbf{Z}_C$ and it produces no reflection [6, Sec. II], [7], [8, Sec. 9].

If a diagonalization of the matrix $\mathbf{Y}'\mathbf{Z}'$ produces a matrix $\mathbf{T}$ satisfying the first line of (3), we find that two possible solutions of the second line of (3) are

$$\mathbf{S} = {}^t\mathbf{T}^{-1} \tag{16}$$

where ${}^t\mathbf{A}$ is used to denote the transpose of a matrix $\mathbf{A}$, and

$$\mathbf{S} = j\omega c_K \mathbf{Y}'^{-1}\mathbf{T} \tag{17}$$

where c_K is an arbitrary scalar different from zero, which may depend on frequency, and which has the dimensions of p.u.l. capacitance [11, eq. (19c)], [12], [13], [14, Appendix]. When $\mathbf{S}$ and $\mathbf{T}$ are defined by (3) and (16), we say that they are biorthonormal, and that the eigenvectors contained in $\mathbf{S}$ and $\mathbf{T}$ (i.e., their column vectors) are biorthonormal. When $\mathbf{S}$ and $\mathbf{T}$ are defined by (3) and (17), we say that they are associated, and that the eigenvectors contained in $\mathbf{S}$ and $\mathbf{T}$ are associated [1], [6]. For associated eigenvectors, $\mathbf{Z}_{MC}$ is diagonal and given by

$$\mathbf{Z}_{MC} = \frac{1}{j\omega c_K}\Gamma. \tag{18}$$

Thus, for associated eigenvectors, for a wave propagating in a given direction and for any $\alpha \in \{1, \ldots, n\}$, by (13) and (18) we have [1], [6]

$$v_{M\alpha} = \frac{\varepsilon_D}{j\omega c_K}\gamma_\alpha i_{M\alpha} \tag{19}$$

where ε_D is equal to 1 if the wave propagates toward the far end, or to -1 if the wave propagates toward the near end.

From (2) to here, we have only assumed that we use a uniform MTL, that $\mathbf{Z}'$ and $\mathbf{Y}'$ are invertible, and that $\mathbf{Z}'\ \mathbf{Y}'$, or equivalently $\mathbf{Y}'\ \mathbf{Z}'$ is diagonalizable. For a lossless MTL, we can compute a frequency-independent and real (FIR) matrix $\mathbf{T}$ satisfying [15, Sec. 4.4.3]

$$\mathbf{T}^{-1} = \varepsilon_0\ {}^t\mathbf{T}\mathbf{C}'^{-1} \tag{20}$$

where ε_0 is the permittivity of vacuum, and we have

$$\gamma_\alpha = \frac{j\omega}{c_\alpha} \tag{21}$$

where the positive real c_α is the propagation velocity of the mode α. In (20), ε_0 is used to obtain a dimensionless $\mathbf{T}$.

If, looking for associated eigenvectors, we apply (17) with $c_K = \varepsilon_0$ to this $\mathbf{T}$, we obtain a FIR matrix $\mathbf{S}$, and we can easily show that it satisfies (16). Thus, the eigenvectors contained in $\mathbf{S}$ and $\mathbf{T}$ are biorthonormal and associated eigenvectors in this case. These eigenvectors can be used to obtain, for the MTL, an equivalent circuit comprising ideal multiwinding transformers and n uncoupled lossless two-conductor TLs [12].

Based on the fact that we can use a FIR matrix $\mathbf{T}$ or $\mathbf{S}$, we find that $\mathbf{Z}_C$ is FIR for the lossless MTL.

III. Generalized Associated Eigenvectors

A more general possible choice, referred to as generalized associated eigenvectors, is given by

$$\mathbf{S} = j\omega \mathbf{Y}'^{-1} \mathbf{T} \mathbf{c}_K \tag{22}$$

where $\mathbf{c}_K$ is an arbitrary invertible diagonal matrix, possibly frequency-dependent, having the dimensions of p.u.l. capacitance. For generalized associated eigenvectors, $\mathbf{Z}_{MC}$ is a diagonal matrix given by

$$\mathbf{Z}_{MC} = \frac{1}{j\omega} \mathbf{c}_K^{-1} \Gamma. \tag{23}$$

For generalized associated eigenvectors, using (13) and (23), we obtain a result similar to (19)

$$v_{M\alpha} = \frac{\varepsilon_D}{j\omega c_{K\alpha\alpha}} \gamma_\alpha i_{M\alpha} \tag{24}$$

where $c_{K\alpha\beta}$ denotes an entry of $\mathbf{c}_K$.

We say that a total decoupling occurs when a particular choice of $\mathbf{T}$ and $\mathbf{S}$ leads to a diagonal $\mathbf{Z}_{MC}$. In this case, an equivalent circuit comprising voltage-controlled voltage sources, current-controlled current sources, and n uncoupled TLs may be defined for the $(n+1)$-conductor MTL, the αth TL having a propagation constant γ_α and a characteristic impedance equal to the αth diagonal entry of $\mathbf{Z}_{MC}$. We note that this equivalent circuit is different from the abovementioned equivalent circuit using ideal multiwinding transformers, which only applies to lossless MTLs.

We can establish the following result [8, Sec. 7].

Theorem 1: Total decoupling occurs if and only if generalized associated eigenvectors are used.

Proof: By (23), generalized associated eigenvectors provide total decoupling.

Conversely, if total decoupling is achieved, $\Gamma \mathbf{Z}_{MC}^{-1}$ is diagonal. By (12) we have $\mathbf{S} = \mathbf{Y}'^{-1} \mathbf{T} \Gamma \mathbf{Z}_{MC}^{-1}$, which complies with the definition of generalized eigenvectors (22) for $j\omega \mathbf{c}_K = \Gamma \mathbf{Z}_{MC}^{-1}$. ■

The diagonalization of $\mathbf{Y}'\mathbf{Z}'$ and $\mathbf{Z}'\mathbf{Y}'$ in (3) provides a decoupling of (6), leading to (8), but it need not provide total decoupling. For instance, the biorthonormal eigenvectors used by many authors, which satisfy (16) in the place of (17) or (22), are such that total decoupling need not be present, so that it need not lead us to said equivalent circuit [8, Sec. 7].

For most applications of modal vectors, any total decoupling is satisfactory, so that any choice of the invertible diagonal matrix $\mathbf{c}_K$ is acceptable. However, we might want to use biorthonormal eigenvectors providing a total decoupling. Is this possible? The next theorem is new and answers this question.

Theorem 2: If $\mathbf{Z}'\mathbf{Y}'$, or equivalently $\mathbf{Y}'\mathbf{Z}'$, is diagonalizable, there exist $\mathbf{S}$ and $\mathbf{T}$ satisfying (3) such that the eigenvectors contained in $\mathbf{S}$ and $\mathbf{T}$ are biorthonormal and generalized associated eigenvectors.

Proof: Since $\mathbf{Z}'$ is symmetric and invertible, $\mathbf{Z}'^{-1}$ is symmetric and invertible. Since $\mathbf{Z}'\mathbf{Y}'$ is diagonalizable and $\mathbf{Y}'$ is symmetric, we can use the Case II(b) of the [9, Th. 4.5.15] to conclude that there exists a nonsingular matrix $\mathbf{M}$ such that ${}^t\mathbf{M}\ \mathbf{Z}'^{-1}\ \mathbf{M}$ and ${}^t\mathbf{M}\ \mathbf{Y}'\ \mathbf{M}$ are diagonal. Thus, $\mathbf{M}^{-1}\ \mathbf{Z}'\ \mathbf{Y}'\ \mathbf{M}$ is diagonal so that we can use $\mathbf{S} = \mathbf{M}$. Also, ${}^t\mathbf{S}\ \mathbf{Y}'\ \mathbf{S}$ being diagonal, we can define a diagonal matrix $\mathbf{c}_K$ by $j\omega\ \mathbf{c}_K = {}^t\mathbf{S}\ \mathbf{Y}'\ \mathbf{S}$. At this stage, we have found an invertible matrix $\mathbf{S}$ satisfying the second line of (3) and an invertible matrix $\mathbf{c}_K$ such that

$$\mathbf{S} = j\omega \mathbf{Y}'^{-1}\ {}^t\mathbf{S}^{-1} \mathbf{c}_K. \tag{25}$$

Let us use (16) to define $\mathbf{T}$. We see that (22) is satisfied. ■

This theorem extends to lossy MTLs the possibility, established at the end of Section II for a lossless MTL, of obtaining biorthonormal and generalized associated eigenvectors. In the [9, Th. 4.5.15], we observe that the proof of the existence of the nonsingular matrix $\mathbf{M}$ is constructive, and uses Takagi's factorization, which is a special case of the singular value decomposition for symmetric matrices. However, the algorithm used to obtain $\mathbf{M}$ is involved. Since we always want to use generalized associated eigenvectors (to obtain total decoupling) and there is no clear advantage attached to biorthonormal eigenvectors, we do not compute $\mathbf{M}$ to solve an actual problem.

We now disclose another new choice of generalized eigenvectors, which is at the same time simple to compute and very useful.

Theorem 3: For any matrix $\mathbf{T}$ satisfying the first line of (3), a possible choice of generalized associated eigenvectors is given by

$$\mathbf{S} = \frac{1}{z_K} \mathbf{Z}_C \mathbf{T} \tag{26}$$

where z_K is an arbitrary scalar different from zero, which may depend on frequency, and which has the dimensions of impedance.

Proof: Using (14), we get $(1/z_K)\, \mathbf{Z}_C \mathbf{T} = j\omega\ \mathbf{Y}'^{-1}\ \mathbf{T}\, \mathbf{c}_K$ for $j\omega\, \mathbf{c}_K = \Gamma / z_K$. Thus, (22) is satisfied if we use (26). ■

The generalized associated eigenvectors given by (26) have several advantages. The first is that they have a clear physical significance: if we inject a single modal current at the near end of the interconnection whose far end is connected to an $(n+1)$-terminal device presenting an impedance matrix equal to $\mathbf{Z}_C$, we obtain a single modal voltage. A second advantage occurs if we decide that z_K is FIR. In this case, if $\mathbf{Z}_C$ and $\mathbf{S}$ are FIR, then $\mathbf{T}$ is FIR. This property will be used in the next section.

IV. Low- and High-Frequency Approximations

In this section, we want to rigorously derive low- and high-frequency approximations for $\mathbf{Z}_C$ and high-frequency

approximations for $\mathbf{S}$ and $\mathbf{T}$. The difficulty is that small perturbations in a matrix can produce radical changes in its eigenvectors. Thus, much cannot be said about the effect of perturbations in $\mathbf{Z}'$ and $\mathbf{Y}'$ on $\mathbf{S}$ and $\mathbf{T}$, and (14) cannot be used to directly assess the effect of perturbations in $\mathbf{Z}'$ and $\mathbf{Y}'$ on $\mathbf{Z}_C$.

Using the principal matrix square root defined in the Appendix and (3), we can write

$$\sqrt{\mathbf{Z}'\mathbf{Y}'} = \mathbf{S}\Gamma\mathbf{S}^{-1} \quad \text{and} \quad \sqrt{\mathbf{Y}'\mathbf{Z}'} = \mathbf{T}\Gamma\mathbf{T}^{-1} \tag{27}$$

so that by (14), we have

$$\begin{aligned}\mathbf{Z}_C &= \sqrt{\mathbf{Z}'\mathbf{Y}'}^{-1}\mathbf{Z}' = \sqrt{\mathbf{Z}'\mathbf{Y}'}\mathbf{Y}^{-1} \\ &= \mathbf{Y}'^{-1}\sqrt{\mathbf{Y}'\mathbf{Z}'} = \mathbf{Z}'\sqrt{\mathbf{Y}'\mathbf{Z}'}^{-1}.\end{aligned} \tag{28}$$

Using the matrix exponential of a principal matrix square root introduced in the Appendix, a scattering matrix, denoted by $\mathcal{S}(z)$ and defined by [8, Sec. 8]

$$\begin{pmatrix}\mathbf{v}_-(0)\\ \mathbf{v}_+(z)\end{pmatrix} = \mathcal{S}(z)\begin{pmatrix}\mathbf{v}_+(0)\\ \mathbf{v}_-(z).\end{pmatrix} \tag{29}$$

is given by

$$\mathcal{S}(z) = \begin{pmatrix}0 & e^{-z\sqrt{\mathbf{Z}'\mathbf{Y}'}}\\ e^{-z\sqrt{\mathbf{Z}'\mathbf{Y}'}} & 0\end{pmatrix}. \tag{30}$$

A length z of the MTL is completely characterized by $\mathbf{Z}_C$ and $\mathcal{S}(z)$, so that it is also completely characterized by z, $\mathbf{Z}_C$ and by

$$\mathbf{G} = \sqrt{\mathbf{Z}'\mathbf{Y}'} \tag{31}$$

which will be referred to as the lineic propagation matrix because, according to [10, eq. (6.2.36)] it is the opposite of the derivative of the nondiagonal entries of $\mathcal{S}(z)$ with respect to z at $z = 0$ (lineic is a synonym of p.u.l., used in the Electromagnetism chapter of the International Electrotechnical Vocabulary [16]).

The theorem on the continuity of $f(\mathbf{A})$ stated in the Appendix, (28) and (31) allow us to say that a small perturbation in $\mathbf{Z}'$ and/or $\mathbf{Y}'$ will produce a small change in $\mathbf{Z}_C$ and a small change in $\mathbf{G}$. At low frequencies where $\mathbf{Z}'$ is approximately equal to the dc p.u.l. resistance matrix $\mathbf{Z}'_{\mathrm{DC}}$, and $\mathbf{Y}'$ is approximately equal to $j\omega$ times a dc p.u.l. capacitance matrix $\mathbf{C}'_{\mathrm{DC}}$, $\mathbf{Z}_C$ is approximately given by

$$\mathbf{Z}_C \approx \sqrt{j\omega\mathbf{R}'_{\mathrm{DC}}\mathbf{C}'_{\mathrm{DC}}}^{-1}\mathbf{R}'_{\mathrm{DC}} \tag{32}$$

so that

$$\mathbf{Z}_C \approx \frac{1-j}{\sqrt{2\omega}}\mathbf{A}_C \tag{33}$$

where $\mathbf{A}_C$ is a FIR matrix.

At high frequencies, we have $\mathbf{Z}' = j\omega\mathbf{L}'_O + \Delta\mathbf{Z}'$ and $\mathbf{Y}' = j\omega\mathbf{C}'_O + \Delta\mathbf{Y}'$ where $\mathbf{L}'_O$ and $\mathbf{C}'_O$ are frequency independent positive definite real matrices such that $|||\omega\mathbf{L}'_O|||_\infty >> |||\Delta\mathbf{Z}'|||_\infty$ and $|||\omega\mathbf{C}'_O|||_\infty >> |||\Delta\mathbf{Y}'|||_\infty$, where the maximum (absolute) row sum norm $|||\mathbf{A}|||_\infty$ of a matrix $\mathbf{A}$ is a matrix norm defined by [9, Sec. 5.6.5]

$$|||\mathbf{A}|||_\infty = \max_i \sum_{j=1}^{n} \left|[\mathbf{A}]_{ij}\right|. \tag{34}$$

It is possible to define $\mathbf{L}'_O$ as being equal to the high-frequency p.u.l. external inductance matrix. The high-frequency p.u.l. internal impedance matrix of the interconnection being proportional to the square root of frequency for a normal skin effect [17], we find that $|||\Delta\mathbf{Z}'|||_\infty = o(\omega)$ as $\omega \to \infty$. It is possible to define $\mathbf{C}'_O$ such that $\omega\mathbf{C}'_O$ is equal to the imaginary part of $\mathbf{Y}'$ at one of the high frequencies of interest. Since the loss tangent of the dielectrics used in the interconnection must be low at these frequencies (typically below 0.03), the condition $|||\omega\mathbf{C}'_O|||_\infty >> |||\Delta\mathbf{Y}'|||_\infty$ is indeed satisfied.

Thus, removing the second order terms, we get

$$\begin{cases}\mathbf{Z}'\mathbf{Y}' \approx -\omega^2\mathbf{L}'_O\mathbf{C}'_O + j\omega\left(\mathbf{L}'_O\Delta\mathbf{Y}' + \Delta\mathbf{Z}'\mathbf{C}'_O\right)\\ \mathbf{Y}'\mathbf{Z}' \approx -\omega^2\mathbf{C}'_O\mathbf{L}'_O + j\omega\left(\Delta\mathbf{Y}'\mathbf{L}'_O + \mathbf{C}'_O\Delta\mathbf{Z}'\right).\end{cases} \tag{35}$$

We can use diagonalizations of $\mathbf{C}'_O\mathbf{L}'_O$ and $\mathbf{L}'_O\mathbf{C}'_O$ such that

$$\begin{aligned}\mathbf{T}_0^{-1}\mathbf{C}'_O\mathbf{L}'_O\mathbf{T}_0 &= \mathbf{S}_0^{-1}\mathbf{L}'_O\mathbf{C}'_O\mathbf{S}_0 \\ &= \left(\frac{\Gamma_0}{j\omega}\right)^2 = \left(\frac{\mathrm{diag}_n(\gamma_{01},\ldots,\gamma_{0n})}{j\omega}\right)^2\end{aligned} \tag{36}$$

where $\mathbf{T}_0$ and $\mathbf{S}_0$ are FIR [13], [15, Sec. 5.2], $\mathbf{T}_0$ and $\mathbf{S}_0$ containing associated eigenvectors. Using (36) in (35), we get

$$\begin{cases}\mathbf{Z}'\mathbf{Y}' \approx \mathbf{S}_0\{\Gamma_0^2 + j\omega\mathbf{S}_0^{-1}(\mathbf{L}'_O\Delta\mathbf{Y}' + \Delta\mathbf{Z}'\mathbf{C}'_O)\mathbf{S}_0\}\mathbf{S}_0^{-1}\\ \mathbf{Y}'\mathbf{Z}' \approx \mathbf{T}_0\{\Gamma_0^2 + j\omega\mathbf{T}_0^{-1}(\Delta\mathbf{Y}'\mathbf{L}'_O + \mathbf{C}'_O\Delta\mathbf{Z}')\mathbf{T}_0\}\mathbf{T}_0^{-1}.\end{cases} \tag{37}$$

For $\zeta \in [0, 1]$, let us define the function

$$\begin{aligned}\mathbf{A}(\zeta) &= -(1-\zeta)\,\omega^2\mathbf{L}'_O\mathbf{C}'_O + \zeta\,\mathbf{Z}'\mathbf{Y}' \\ &\approx -\omega^2\mathbf{L}'_O\mathbf{C}'_O + \zeta\, j\omega(\mathbf{L}'_O\Delta\mathbf{Y}' + \Delta\mathbf{Z}'\mathbf{C}'_O).\end{aligned} \tag{38}$$

If we apply [10, eq. (6.6.28)] to this function, we obtain

$$\left.\frac{d\sqrt{\mathbf{A}}}{d\zeta}\right|_{\zeta=0} \simeq \mathbf{S}_0\left\{\Delta f \circ \mathbf{S}_0{}^{-1}\left.\frac{d\mathbf{A}}{d\zeta}\right|_{\zeta=0}\mathbf{S}_0\right\}\mathbf{S}_0^{-1} \tag{39}$$

where $\circ$ is the Hadamard product and Δf is the matrix of size $n \times n$ defined by

$$\begin{aligned}[\Delta f]_{\alpha\beta} &= \frac{\gamma_{0\alpha}-\gamma_{0\beta}}{\gamma_{0\alpha}^2-\gamma_{0\beta}^2} = \frac{1}{\gamma_{0\alpha}+\gamma_{0\beta}}, \qquad \text{for } \gamma_{0\alpha} \neq \gamma_{0\beta} \\ [\Delta f]_{\alpha\beta} &= \frac{1}{2\gamma_{0\alpha}}, \qquad \text{for } \gamma_{0\alpha} = \gamma_{0\beta}.\end{aligned} \tag{40}$$

By (31) and (38), we have

$$\mathbf{G} = \sqrt{\mathbf{A}(1)} \approx \sqrt{\mathbf{A}(0)} + \left.\frac{d\sqrt{\mathbf{A}}}{d\zeta}\right|_{\zeta=0}. \tag{41}$$

Using (38), (39), and (41), we find that $\mathbf{G}$ is approximately given by

$$\begin{aligned}\mathbf{G} \;&\simeq j\omega\sqrt{\mathbf{L}'_O\mathbf{C}'_O} \\ &\quad + j\omega\mathbf{S}_0\left\{\Delta f \circ \mathbf{S}_0^{-1}(\mathbf{L}'_O\Delta\mathbf{Y}' + \Delta\mathbf{Z}'\mathbf{C}'_O)\mathbf{S}_0\right\}\mathbf{S}_0^{-1}.\end{aligned} \tag{42}$$

By (28) and (31), we have $\mathbf{Z}_C = \mathbf{G}\ \mathbf{Y}'^{-1}$. Using [9, Sec. 5.6.16] and dropping the second order term, we obtain

$$\begin{aligned}\mathbf{Z}_C \approx\; &\sqrt{\mathbf{L}'_O\mathbf{C}'_O}\mathbf{C}'^{-1}_O \\ &+ \mathbf{S}_0\left\{\Delta f \circ \mathbf{S}_0^{-1}(\mathbf{L}'_O\Delta\mathbf{Y}' + \Delta\mathbf{Z}'\mathbf{C}'_O)\mathbf{S}_0\right\}\mathbf{S}_0^{-1}\mathbf{C}'^{-1}_O \\ &- \frac{1}{j\omega}\sqrt{\mathbf{L}'_O\mathbf{C}'_O}\mathbf{C}'^{-1}_O\Delta\mathbf{Y}'\mathbf{C}'^{-1}_O.\end{aligned} \tag{43}$$

From the previous discussion of $|||\Delta\mathbf{Z}'|||_\infty$ and $|||\Delta\mathbf{Y}'|||_\infty$ and the fact that $\Delta f \propto 1/j\omega$, we find that, at some high frequencies, we can keep only the first term in (42) and (43). Thus, $\mathbf{Z}_C$ gets close to the FIR matrix

$$\mathbf{Z}_{C0} = \sqrt{\mathbf{L}'_O\mathbf{C}'_O}\,\mathbf{C}'^{-1}_O \tag{44}$$

and $\mathbf{G}$ is near to the imaginary matrix

$$\mathbf{G}_0 = j\omega\sqrt{\mathbf{L}'_O\mathbf{C}'_O} = \mathbf{S}_0\Gamma_0\mathbf{S}_0^{-1}. \tag{45}$$

We want now to find approximate models of the interconnection, for which the characteristic impedance matrix is FIR and for which the transition matrices from modal variables to natural variables can be chosen to be FIR matrices containing generalized associated eigenvectors. In a way, we want to trade the accuracy of our original MTL model for a simplification.

Thus, let us consider a second MTL having a characteristic impedance matrix equal to $\mathbf{Z}_{C0}$ and a lineic propagation matrix equal to $\mathbf{G}_0$. According to our discussion, this MTL can be used to model our interconnection at high frequencies. By (28) and (31), the p.u.l. impedance matrix and the p.u.l. admittance matrix of the second MTL are $j\omega\mathbf{L}'_O$ and $j\omega\mathbf{C}'_O$, respectively. Thus, we can use $\mathbf{S}_0$ and $\mathbf{T}_0$ as transition matrices from modal variables to natural variables. We see that, in the second MTL, the desired simplification has been obtained, but all losses are neglected. The second MTL is, therefore, not satisfactory for most on-package and on-chip interconnections, since we know that losses often play an important role in their behavior at high frequency.

To obtain a better approximation, we can define a third MTL having a characteristic impedance matrix $\mathbf{Z}_{C3}$ exactly given by the right-hand side of (43) and a lineic propagation matrix $\mathbf{G}_3$ exactly given by the right-hand side of (42). However, $\mathbf{Z}_{C3}$ and the transition matrices from modal variables to natural variables, denoted by $\mathbf{S}_3$ and $\mathbf{T}_3$, need not be FIR, because the curly bracket in (42) and (43) need not be diagonal or real. Thus, the third MTL enhances the accuracy as compared to the second MTL since it is correct to the first order in $\Delta\mathbf{Z}'$ and $\Delta\mathbf{Y}'$, but it does not have the property that we are looking for.

We therefore try a different approach, according to which we define a fourth MTL having a characteristic impedance matrix equal to $\mathbf{Z}_{C0}$ and a lineic propagation matrix given by

$$\mathbf{G}_4 = \mathbf{S}_0\,\mathrm{Diag}(\mathbf{S}_0^{-1}\mathbf{G}\mathbf{S}_0)\mathbf{S}_0^{-1} \tag{46}$$

where, for a square matrix $\mathbf{A}$, $\mathrm{Diag}(\mathbf{A})$ denotes the diagonal matrix having the same diagonal entries as $\mathbf{A}$. A part of the effects of losses is lost in $\mathbf{G}_4$ but a remaining part is not. Let us use $\mathbf{Z}'_4$ to denote the p.u.l. impedance matrix of the fourth MTL, and $\mathbf{Y}'_4$ to denote its p.u.l. admittance matrix. By (28) and (31), we have

$$\begin{cases}\mathbf{Z}'_4 = \mathbf{G}_4\mathbf{Z}_{C0}\\ \mathbf{Y}'_4 = \mathbf{Z}_{C0}^{-1}\mathbf{G}_4.\end{cases} \tag{47}$$

Using (46), we obtain

$$\mathbf{Z}'_4\mathbf{Y}'_4 = \mathbf{S}_0\left[\mathrm{Diag}(\mathbf{S}_0^{-1}\mathbf{G}\mathbf{S}_0)\right]^2\mathbf{S}_0^{-1} \tag{48}$$

TABLE I
FOUR MODELS CONSIDERED IN SECTION IV

Name	Matrices	Accuracy
First MTL	$\mathbf{Z}_C$ need not be FIR	Exact
	G need not be FIR	
	$\mathbf{S}$, $\mathbf{T}$ need not be FIR	
Second MTL	$\mathbf{Z}_{C0}$ is FIR	Low
	$\mathbf{G}_0$ is FIR	
	$\mathbf{S}_0$, $\mathbf{T}_0$ are FIR	
Third MTL	$\mathbf{Z}_{C3}$ need not be FIR	High (see Section V)
	$\mathbf{G}_3$ need not be FIR	
	$\mathbf{S}_3$, $\mathbf{T}_3$ need not be FIR	
Fourth MTL	$\mathbf{Z}_{C0}$ is FIR	Medium (see Section V)
	$\mathbf{G}_4$ need not be FIR	
	$\mathbf{S}_0$, $\mathbf{T}_4$ are FIR	

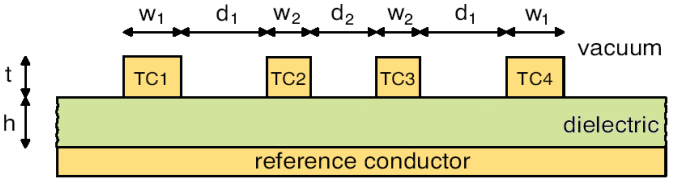

Fig. 2. Cross section of a multiconductor microstrip interconnection comprising $n = 4$ TCs and a GC.

and

$$\mathbf{Y}'_4\mathbf{Z}'_4 = \mathbf{Z}_{C0}^{-1}\mathbf{S}_0\left[\mathrm{Diag}(\mathbf{S}_0^{-1}\mathbf{G}\mathbf{S}_0)\right]^2\mathbf{S}_0^{-1}\mathbf{Z}_{C0}. \tag{49}$$

Thus, for the fourth MTL, a possible transition matrix from modal voltages to natural voltages is $\mathbf{S}_0$ and a possible FIR transition matrix from modal currents to natural currents is given by

$$\mathbf{T}_4 = z_K\mathbf{Z}_{C0}^{-1}\mathbf{S}_0 = z_K\,j\omega\mathbf{C}'_0\mathbf{S}_0\Gamma_0^{-1} \tag{50}$$

where z_K is an arbitrary FIR impedance, and where we have used (14) applied to the second MTL.

Thus, we have obtained an approximate model which does not neglect losses, for which the characteristic impedance matrix is FIR and for which $\mathbf{S}_0$ and $\mathbf{T}_4$ are FIR transition matrices from modal variables to natural variables which, according to Theorem 3, contain generalized associated eigenvectors. Also, (44) and (50) show that losses are ignored in the computation of $\mathbf{Z}_{C0}$, $\mathbf{S}_0$, and $\mathbf{T}_4$. Table I summarizes the properties of the models considered in this section, and their expected accuracy at high frequency.

V. COMPARISON OF HIGH-FREQUENCY APPROXIMATIONS

We now want to compare the accuracy of the second, third, and fourth MTL defined in Section IV as approximate models of an interconnection. For this comparison, we consider a multiconductor microstrip interconnection shown in Fig. 2, built in the substrate of an MCM-L, with the parameters $t = w_1 = w_2 = h = d_1 = d_2 = 50\ \mu$m. To obtain the p.u.l. impedance of this interconnection, we have used the analytical

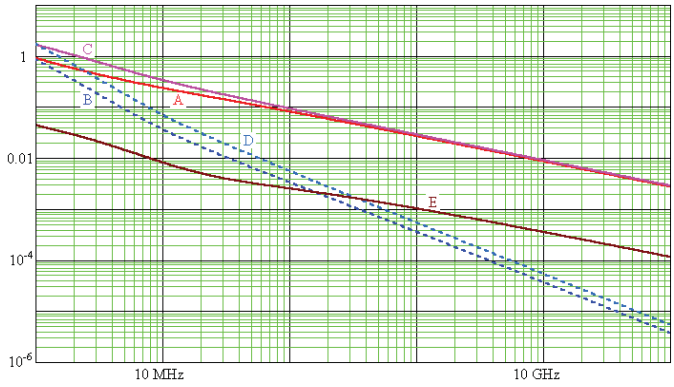

Fig. 3. Taking only resistive losses into account. Curve A: error of $\mathbf{Z}_{C0}$. Curve B: error of $\mathbf{Z}_{C3}$. Curve C: error of $\mathbf{G}_0$. Curve D: error of $\mathbf{G}_3$. Curve E: error of $\mathbf{G}_4$.

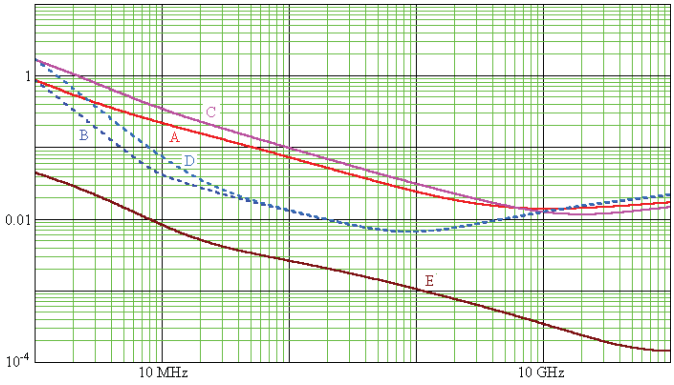

Fig. 4. Taking resistive and dielectric losses into account. Curve A: error of $\mathbf{Z}_{C0}$. Curve B: error of $\mathbf{Z}_{C3}$. Curve C: error of $\mathbf{G}_0$. Curve D: error of $\mathbf{G}_3$. Curve E: error of $\mathbf{G}_4$.

resistive loss model described in [17]. This model uses the p.u.l. external inductance matrix, denoted by $\mathbf{L}'_0$, the matrix of the equivalent inverse widths of the TCs, and the matrix of the equivalent inverse widths of the GC, all of which have been computed for this configuration [18, Sec. VII]. To obtain the p.u.l. admittance of this interconnection, we have used the second model described in [19], according to which the complex permittivity is a logarithm of a bilinear function of the Laplace variable. This model was used with parameters corresponding to a high-speed multifunctional epoxy laminate, in which the relative permittivity is $3.39–0.037\,j$ at 1 GHz. The resulting MTL model of the interconnection is such that $\mathbf{S}$, $\mathbf{T}$, and $\mathbf{Z}_C$ are frequency dependent.

We have studied the approximations of Section IV, for which we have used $\mathbf{L}'_O = \mathbf{L}'_0$ and $\mathbf{C}'_O$ such that $\omega\mathbf{C}'_O$ is equal to the imaginary part of $\mathbf{Y}'$ at 1 GHz. We have considered the error in the approximation of several matrices, where the error of a matrix $\mathbf{A}$ is defined as

$$e(\mathbf{A}) = \frac{|||\mathbf{A} - \mathbf{A}_E|||_\infty}{|||\mathbf{A}_E|||_\infty} \tag{51}$$

where $\mathbf{A}_E$ is the exact value of $\mathbf{A}$.

Taking only resistive losses into account, we have obtained the results shown in Fig. 3 for the errors of $\mathbf{Z}_{C0}$, of $\mathbf{Z}_{C3}$, of $\mathbf{G}_0$, of $\mathbf{G}_3$, and of $\mathbf{G}_4$. Here, the fact that $|||\Delta\mathbf{Z}'|||_\infty = o(\omega)$ as $\omega \to \infty$ entails that the errors vanish as $\omega \to \infty$. The fact that, at high frequencies, the errors of $\mathbf{Z}_{C3}$ and of $\mathbf{G}_3$ are much smaller than the errors of $\mathbf{Z}_{C0}$ and of $\mathbf{G}_0$, respectively, indicates that (42) and (43) provide an increased accuracy compared to the first term of their right-hand sides. At every frequency shown, the error of $\mathbf{G}_4$ is more than one order of magnitude smaller than the errors of $\mathbf{G}_0$. These results agree with the last column of Table I.

Taking all losses into account, we have obtained the results shown in Fig. 4 for the errors of $\mathbf{Z}_{C0}$, $\mathbf{Z}_{C3}$, $\mathbf{G}_0$, $\mathbf{G}_3$, and $\mathbf{G}_4$. Here, our choice of $\mathbf{C}'_O$ is such that $|||\Delta\mathbf{Y}'|||_\infty$ reaches a minimum near 1 GHz, so that we observe that the errors of $\mathbf{Z}_{C3}$ and of $\mathbf{G}_3$ reach a minimum near 1 GHz. Again, at every frequency shown, the error of $\mathbf{G}_4$ is more than one order of magnitude smaller than the errors of $\mathbf{G}_0$.

If we are interested in the characteristic impedance matrix, the accuracy of the third MTL, which uses $\mathbf{Z}_{C3}$, is higher than that of the second and fourth MTLs, which both use $\mathbf{Z}_{C0}$. In fact, we see that $\mathbf{Z}_{C3}$ given by (43) can be used to assess $e(\mathbf{Z}_C)$ at high frequencies, for the second and fourth MTLs. We obtain (52), shown at the bottom of the page, which is valid without upper frequency limit if $\Delta\mathbf{Y}' = 0$, or at least up to the frequency at which $\omega\mathbf{C}'_O$ is equal to the imaginary part of $\mathbf{Y}'$, in the case where $\Delta\mathbf{Y}' \neq 0$. In Figs. 3 and 4, the domain of validity of (52) is the frequency interval where the curve B is well below the curve A.

If we are interested in the lineic propagation matrix, the accuracy of the third and fourth MTLs, which uses $\mathbf{G}_3$ and $\mathbf{G}_4$, respectively, is higher than that of the second MTL, which uses $\mathbf{G}_0$. However, Figs. 3 and 4 show that the third MTL is not clearly always better or worse than the fourth MTL, which uses $\mathbf{G}_4$.

We are now interested in the characteristics of the different MTL models with respect to the simulation of a link. We have computed the signals at the ends of a 20-mm-long section of the interconnection, used in a conventional single-ended signaling configuration in which each end sees an impedance matrix of 50 $\Omega \times \mathbf{1}_n$ with respect to the GC, where $\mathbf{1}_n$ is the identity matrix of size $n \times n$. A comparison of the exact MTL model with the second MTL model (lossless) is shown in Fig. 5. The inaccuracy of the second MTL model is visible above 5 GHz. A comparison of the exact MTL model with the fourth MTL model is shown in Fig. 6. In this case, no difference between the computed voltages is visible above 2 GHz because the high frequency losses are accurately accounted for.

The example considered in this section and the theory of Section IV allows us to write that, for the types of

$$e(\mathbf{Z}_{C0}) \approx \frac{\left|\left|\left|\mathbf{S}_0\left\{\Delta f \circ \mathbf{S}_0^{-1}(\mathbf{L}'_O\Delta\mathbf{Y}' + \Delta\mathbf{Z}'\mathbf{C}'_O)\mathbf{S}_0\right\}\mathbf{S}_0^{-1}\mathbf{C}'^{-1}_O - \frac{1}{j\omega}\sqrt{\mathbf{L}'_O\mathbf{C}'_O}\mathbf{C}'^{-1}_O\Delta\mathbf{Y}'\mathbf{C}'^{-1}_O\right|\right|\right|_\infty}{\left|\left|\left|\sqrt{\mathbf{L}'_O\mathbf{C}'_O}\mathbf{C}'^{-1}_O\right|\right|\right|_\infty} \tag{52}$$

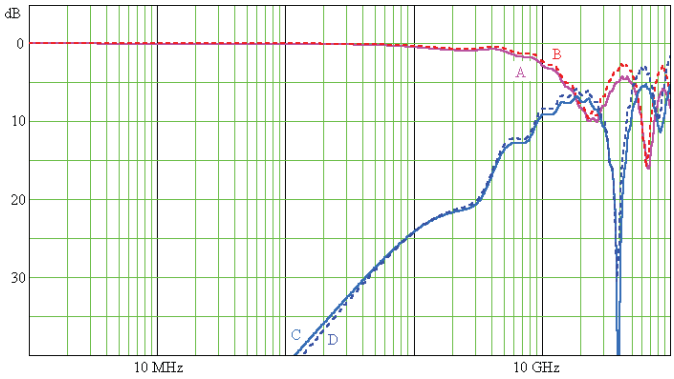

Fig. 5. Attenuations at the far end when a signal is applied at the near end of TC2. Curve A: exact signal on TC2. Curve B: signal on TC2 according to the second MTL model. Curve C: exact signal on TC3. Curve D: signal on TC3 according to the second MTL model.

Fig. 6. Attenuations at the far end when a signal is applied at the near end of TC2. Curve A: exact signal on TC2. Curve B: signal on TC2 according to the fourth MTL model. Curve C: exact signal on TC3. Curve D: signal on TC3 according to the fourth MTL model.

interconnection considered in this paper:

1) it is usually possible to consider that, in a band of the highest frequencies of interest, losses can be ignored in the computation of the characteristic impedance matrix and of transition matrices from modal electrical variables to natural electrical variables, so as to obtain FIR matrices;
2) this assumption does not necessarily lead us to an MTL model in which losses are ignored or inaccurately accounted for in said frequency band;
3) this assumption is not in contradiction with the fact that the attenuation of transmitted signals is higher at high frequencies;
4) moreover, it is possible to require that said transition matrices from modal electrical variables to natural electrical variables contain FIR generalized associated eigenvectors.

VI. Conclusion

In this paper, we presented several additions to MTL theory, which are needed to explain modal transmission schemes.

In each channel of a link using modal transmission, a modal voltage and a modal current are used for signal transmission, instead of a natural voltage and a natural current in single-ended signaling. This is because the modal variables are expected to propagate like a voltage and a current in an isolated two-conductor TL, hence without crosstalk. We have shown that this total decoupling occurs, and only occurs, with generalized associated eigenvectors.

We have also explored high-frequency approximations. This has allowed us to justify an assumption commonly used in the design of a modal link: an approximate model of the interconnection, which accurately takes high-frequency losses into account, can use a characteristic impedance matrix and a transition matrix from modal electrical variables to natural electrical variables which are computed as if losses were not present. Our justification is not a general proof of the assumption, so that the validity of the approximate model should be considered on a case-by-case basis, for instance using the ex-ante approach proposed in Section V or an ex-post performance analysis of the modal link synthesis based on the assumption.

Appendix

Primary Matrix Functions

Let $\mathbf{A}$ be a diagonalizable matrix of size $n \times n$ and let $\mathbf{A} = \Sigma \Lambda \Sigma^{-1}$ be any diagonalization of $\mathbf{A}$ with $\Lambda = \mathrm{diag}_n(\lambda_1, \ldots, \lambda_n)$. Let $f(u)$ be a continuous scalar-valued function of a real or complex variable u, defined at each λ_α, for $\alpha \in \{1, \ldots, n\}$. The matrix-valued function $f(\mathbf{A})$ given by

$$f(\mathbf{A}) = \mathbf{\Sigma}\, \mathrm{diag}_n\left(f(\lambda_1), \ldots, f(\lambda_n)\right)\, \mathbf{\Sigma}^{-1} \tag{53}$$

is independent of the diagonalization used to represent $\mathbf{A}$. This definition can be extended to nondiagonalizable matrices, if $f(u)$ is smooth enough near the spectrum of $\mathbf{A}$ [10, Sec. 6.2.4]. $f(\mathbf{A})$ commutes with any matrix that commutes with $\mathbf{A}$. $f(\mathbf{A})$ is the primary matrix function associated with $f(u)$, and $f(u)$ is referred to as the stem function of $f(\mathbf{A})$.

A theorem on the continuity of $f(\mathbf{A})$ reads as follows. Let $\mathrm{D} \subset \mathbb{C}$ be a simply connected open set. Let $\mathcal{D}_n(\mathrm{D})$ be the set of the matrices of size $n \times n$ having all their eigenvalues in D. Let $f(u)$ be a scalar-valued analytic function on D. $f(\mathbf{A})$ is continuous on $\mathcal{D}_n(\mathrm{D})$ [10, Sec. 6.2.27].

Using $\sqrt{u}$ to denote the principal square root of $u \in \mathbb{C}$ and $f(u) = \sqrt{u}$ as stem function, we define $f(\mathbf{A}) = \sqrt{\mathbf{A}}$ for a nonsingular matrix $\mathbf{A}$ [10, Sec. 6.2.14]. This primary matrix function can be referred to as principal matrix square root. It can be shown that [10, Sec. 6.2.10]

$$\sqrt{\mathbf{A}}^2 = \sqrt{\mathbf{A}}\sqrt{\mathbf{A}} = \mathbf{A}. \tag{54}$$

However, for two invertible matrices $\mathbf{A}$ and $\mathbf{B}$, there is no simple general relationship between $\sqrt{\mathbf{AB}}$ as a function of $\sqrt{\mathbf{A}}\sqrt{\mathbf{B}}$ or of $\sqrt{\mathbf{B}}\sqrt{\mathbf{A}}$. For any matrix $\mathbf{A}$, using $g(u) = e^u$ as stem function, we define $g(\mathbf{A}) = e^{\mathbf{A}}$. This primary matrix function is referred to as matrix exponential. It can be shown that [10, Sec. 6.2.38]

$$e^{-\mathbf{A}} = (e^{\mathbf{A}})^{-1} \quad \text{and} \quad e^{p\mathbf{A}} = (e^{\mathbf{A}})^P \tag{55}$$

where p is any integer. For a nonsingular matrix $\mathbf{A}$, $g(f(\mathbf{A})) = e^{\sqrt{\mathbf{A}}}$ is defined, and by [10, Sec. 6.2.11] it is the primary matrix function associated with $g(f(u)) = e^{\sqrt{u}}$.

REFERENCES

[1] F. Broydé and E. Clavelier, "A modal transmission technique providing a large reduction of crosstalk and echo," in *Proc. 16th Int. Zurich Symp. Electromagn. Compat.*, Feb. 2005, pp. 341–346.

[2] J. R. Carson and R. S. Hoyt, "Propagation of periodic currents over a system of parallel wires," *Bell Syst. Technol. J.*, vol. 6, no. 3, pp. 495–545, Jul. 1927.

[3] F. Broydé and E. Clavelier, "Crosstalk in balanced interconnections used for differential signal transmission," *IEEE Trans. Circuits Syst. I, Reg. Papers*, vol. 54, no. 7, pp. 1562–1572, Jul. 2007.

[4] S. H. Hall and H. L. Heck, *Advanced Signal Integrity for High-Speed Digital Designs*. New York: Wiley, 2009.

[5] F. Broydé, "Clear as a bell [controlling crosstalk in uniform interconnections]," *IEEE Circuits Devices Mag.*, vol. 20, no. 6, pp. 29–37, Dec. 2004.

[6] F. Broydé and E. Clavelier, "A new method for the reduction of crosstalk and echo in multiconductor interconnections," *IEEE Trans. Circuits Syst. I, Reg. Papers*, vol. 52, no. 2, pp. 405–416, Feb. 2005.

[7] F. Broydé and E. Clavelier, "Corrections to 'A new method for the reduction of crosstalk and echo in multiconductor interconnections,'" *IEEE Trans. Circuits Syst. I, Reg. Papers*, vol. 53, no. 8, p. 1851, Aug. 2006.

[8] F. Broydé and E. Clavelier, *Tutorial on Echo and Crosstalk in Printed Circuit Boards and Multi-Chip Modules—Lecture Slides*, 2nd ed. Maule, France: Excem, Feb. 2012.

[9] R. A. Horn and C. R. Johnson, *Matrix Analysis*. Cambridge, U.K.: Cambridge Univ. Press, 1985.

[10] R. A. Horn and C. R. Johnson, *Topics in Matrix Analysis*. Cambridge, U.K.: Cambridge Univ. Press, 1991.

[11] H. W. Dommel, "Digital computer solution of electromagnetic transients in single- and multiphase networks," *IEEE Trans. Power App. Syst.*, vol. 88, no. 4, pp. 388–399, Apr. 1969.

[12] F.-Y. Chang, "Transient analysis of lossless coupled transmission lines in a nonhomogeneous dielectric medium," *IEEE Trans. Microw. Theory Tech.*, vol. 18, no. 9, pp. 616–626, Sep. 1970.

[13] K. D. Marx, "Propagation modes, equivalent circuits, and characteristic terminations for multiconductor transmission lines with inhomogeneous dielectrics," *IEEE Trans. Microw. Theory Tech.*, vol. 21, no. 7, pp. 450–457, Jul. 1973.

[14] H. W. Dommel and W. S. Meyer, "Computation of electromagnetic transients," *Proc. IEEE*, vol. 62, no. 7, pp. 983–993, Jul. 1974.

[15] C. R. Paul, *Analysis of Multiconductor Transmission Lines*. New York: Wiley, 1994.

[16] *International Electrotechnical Vocabulary—Part 121: Electromagnetism*, IEC Standard 60050-121, 1998.

[17] F. Broydé and E. Clavelier, "An analytical resistive loss model for multiconductor transmission lines and the proof of its passivity," in *Proc. 10th Int. Symp. Electromagn. Compat., EMC Eur. 2011,*, Oct. 2011, pp. 119–122.

[18] F. Broydé and E. Clavelier, "A computation of the high-frequency per-unit-length resistance matrix of a multiconductor interconnections," in *Proc. 10th Int. Symp. Electromagn. Compat.*, Sep. 2011, pp. 351–356.

[19] A. R. Djordjević, R. M. Biljić, V. D. Likar-Smiljanić, T. K. Sarkar, "Wideband frequency-domain characterization of FR-4 and time-domain causality," *IEEE Trans. Electromagn. Compat.*, vol. 43, no. 4, pp. 662–667, Nov. 2001.

Frédéric Broydé (S'84–M'86–SM'01) was born in France in 1960. He received the M.S. degree in physics engineering from the Ecole Nationale Supérieure d'Ingénieurs Electriciens de Grenoble, Grenoble, France, in 1984, and the Ph.D. degree in microwaves and microtechnologies from the Université des Sciences et Technologies de Lille, Lille, France, in 2004.

He co-founded the Excem Corporation, Maule, France, in May 1988, a company providing engineering and research and development services, where he is currently the President and a CTO. His current research interests include multiconductor transmission line theory, development of advanced schemes for high data rate interconnections, and wireless transmission systems. He is a radio amateur (F5OYE). He has authored or co-authored over 85 technical papers, and he is designated as inventor in patent applications of about 55 patent families, for which 21 U.S. patents have been granted up to now.

Evelyne Clavelier (S'84–M'85–SM'02) was born in France in 1961. She received the M.S. degree in physics engineering from the Ecole Nationale Supérieure d'Ingénieurs Electriciens de Grenoble, Grenoble, France.

She is a Co-founder of Excem Corporation, Maule, France, where she is currently the CEO. She is the Manager of Eurexcem (a subsidiary of Excem) and the President of Tekcem, Maule, a company selling or licensing intellectual property rights. Her current research interests include signal integrity. She is involved in research on new models for multiconductor interconnections and on the simulation of modal and pseudodifferential transmission schemes. She is a radio amateur. She is the author or co-author of over 65 technical papers.